Image Sequence Restoration: A PDE Based Coupled Method for Image Restoration and Motion Segmentation

Pierre Kornprobst, Rachid Deriche, G. Aubert

INSTITUT NATIONAL DE RECHERCHE EN INFORMATIQUE ET EN AUTOMATIQUE

Image Sequence Restoration: A PDE based coupled method for image restoration and motion segmentation

P. Kornprobst, R. Deriche and G. Aubert

N° 3308

Novembre 1997

THÈME 3

Rapport de recherche

ISSN 0249-6399

Image Sequence Restoration: A PDE based coupled method for image restoration and motion segmentation

P. Kornprobst, R. Deriche and G. Aubert

Thème 3 — Interaction homme-machine,
images, données, connaissances
Projet ROBOTVIS

Rapport de recherche n° 3308 — Novembre 1997 — 19 pages

Abstract: There is a strong need to automatically remove noise and degradations from noisy image sequences. Applications areas include Image surveillance, Forensic Image Processing, Digital video broadcasting, Digital Film Restoration, Virtual Studio, Medical Image Processing, Remote Sensing .... Image sequence restoration is tightly coupled to motion segmentation. It requires to extract moving objects in order to separately restore the background and each moving region along its particular motion trajectory. Most of the work done to date mainly involves motion compensated temporal filtering techniques with appropriate 2D or 3D Wiener filter for noise suppression, 2D/3D median filtering or more appropriate morphological operators for removing impulsive noise. Usually, motion segmentation and image restoration are tackled separately in image sequence restoration. In this article, the motion segmentation and the image restoration parts are done in a coupled way, allowing the motion segmentation part to positively influence the restoration part and vice-versa. This is the key of our approach that allows to deal simultaneously with the problem of restoration and motion segmentation. To take into account both requirements, we present an original PDE based method which permits to solve the two problems in a coupled way. This PDE based approach allows to anisotropically restore the image sequence: edges are well preserved and blur is not introduced during the restoration process. To this end, we reformulate the image sequence restoration problem as an energy functional minimization. A suitable numerical scheme based on half-quadratic minimization is proposed and its stability demonstrated. Experimental results obtained on noisy synthetic data and real images will illustrate the capabilities of this original and efficient approach.

Key-words: Sequence image restoration, motion segmentation, discontinuity preserving regularization, variational approaches.

Unité de recherche INRIA Sophia Antipolis
2004, route des Lucioles, B.P. 93, 06902 Sophia Antipolis Cedex (France)
Téléphone : 04 93 65 77 77 - International : +33 4 93 65 77 77 — Fax : 04 93 65 77 65 - International : +33 4 93 65 77 65
à partir du 01/01/1998
Téléphone : 04 92 38 77 77 - International : +33 4 92 38 77 77 — Fax : 04 92 38 77 65 - International : +33 4 92 38 77 65

Restauration de séquence d'images: Une méthode couplée à base d'EDP pour la restauration d'image et la segmentation du mouvement

Résumé : Force est de constater la grande nécessité d'éliminer de manière automatique le bruit et les dégradations dans une séquence d'images. Les domaines d'applications sont divers et variés et comprennent la surveillance de sites, l'analyse d'image appliquée au domaine judiciaire, la transmission d'images vidéo, la restauration digitale de films, les studios virtuels, l'imagerie médicale, l'imagerie satellitaire, ... La restauration de séquence d'images est par ailleurs étroitement liée à la segmentation au sens du mouvement. Elle nécessite l'extraction des objets en mouvement de manière à restaurer séparement le fond de l'image et chaque objet en mouvement le long de ses trajectoires. La plupart des travaux effectués à ce jour sont à base d'utilisation de filtres temporels avec compensation de mouvement, de filtres de Wiener 2D ou 3D pour l'élimination du bruit, de filtres médian 2D ou 3D ou d'opérateurs morphologiques plus adaptés pour supprimer le bruit impulsionel. Habituellement, la segmentation au sens du mouvement et la restauration de la séquence sont traitées séparément. Dans cet article, les deux problèmes sont considérées de manière couplées, permettant la segmentation au sens du mouvement d'influencer positivement la restauration et inversement. C'est l'idée maîtresse de notre approche qui permet de traiter simultanément la restauration et la segmentation de séquence d'images. Pour prendre en compte les deux exigences, nous présentons une méthode à base d'Equations aux Dérivées Partielles. Cette approche par EDP permet de restaurer de manière anisotrope la séquence: les contours sont bien conservés et aucun flou n'est introduit. Pour ce faire, on reformule le problème sous forme d'approche variationelle avec minimisation d'énergie. Un algorithme adapté basé sur la minimisation semi-quadratique est proposé et sa stabilité est démontrée. Plusieurs résultats expérimentaux obtenus sur des données synthétiques et réelles illustrent les performances réelles de cette approche originale.

Mots-clés : Restauration de séquences d'images, segmentation du mouvement, régularisation avec préservation des discontinuités, approches variationnelles.

1 Aim and difficulties

Automatic image sequence restoration is clearly a very important problem. Applications areas include Image surveillance, Forensic Image Processing, Digital video broadcasting, Digital Film Restoration, Virtual Studio, Medical Image Processing, Remote Sensing ... See, for example, the recent work done within the European projects,fully or in part, involved with this important problem *AURORA*, *NOBLESSE*, *LIMELIGHT*, *IMPROOFS*,..). Image sequence restoration is tightly coupled to motion segmentation. It requires to extract moving objects in order to separately restore the background and each moving region along its particular motion trajectory. Most of the work done to date mainly involves motion compensated temporal filtering techniques with appropriate 2D or 3D Wiener filter for noise suppression, 2D/3D median filtering or more appropriate morphological operators for removing impulsive noise ([6, 17, 18, 15, 13, 23, 8, 7]). However, and due to the fact that image sequence restoration is an emerging domain compared to 2D image restoration, the literature is not so abundant than the one related to the problem of restoring just a single image. For example, numerous PDE based algorithms have been recently proposed to tackle the problems of noise removal, 2D image enhancement and 2D image restoration in real images with a particular emphasis on preserving the grey level discontinuities during the enhancement/restoration process. These methods, which have been proved to be very efficient, are based on evolving nonlinear partial differential equations (PDE's) (Perona & Malik [26], Nordström [24], Shah [30], Osher & Rudin [28],Proesman *et al.* [27], Cottet and Germain, Alvarez *et al* [2, 3], Cohen [9], Weickert, [31], Malladi & Sethian [22], Aubert *et al.* [4], You *et al.*[33], Sapiro *et al.*[29], Kornprobst & Deriche [20, 19]...)

It is the aim of this article to tackle the important problem of image sequence restoration by applying this PDE based methodology, which has been proved to be very successful in anisotropically restoring images. Therefore, considering the case of an image sequence with some moving objects, we have to consider both motion segmentation and image restoration problems. Usually, these two problems are tackled separately in image sequence restoration. However, it is clear that these two problems must be tackled simultaneously in order to achieve better results. In this article, the motion segmentation and the image restoration parts are done in a coupled way, allowing the motion segmentation part to positively influence the restoration part and vice-versa. This is the key of our approach that allows to deal simultaneously with the problem of restoration and motion segmentation. To take into account both requirements, we present an original PDE based method which permits to solve the two problems in a coupled way, while preserving the discontinuities during the restoration process. We reformulate the problem as an energy functional minimization. A suitable numerical scheme based on half quadratic minimization is also proposed and its stability demonstrated. Results on synthetic and real scene will illustrate the capabilities of this original and efficient approach.

The organization of the article is as follows. In section 2, we make some precise recalls about one of our previous approach for denoising a single image [10, 4, 20] and present our new *divergence operator* discretization scheme. The formalism, the methods and the discretization scheme introduced will be very useful in the sequel. Section 3 is then devoted to presentation of our new approach to deal with the case of noisy images sequence. The precise algorithm will be also given and justified. Experimental results obtained on noisy synthetic and real data will then illustrate the capabilities of this new approach in Section 4. A conclusion is then given in Section 5.

2 A variational method for image restoration

In section 2.1, we recall a classical method in image restoration formulated as a minimization problem [10, 5, 4]. Section 2.2 presents a suitable algorithm based on the introduction of an extended problem. We will detail and propose a generalization of the classical discretization[26] of the equation which will be used in the sequel.

2.1 A classical approach for image restoration

Let $N(x, y)$ be a given noisy image defined for $(x, y) \in \Omega$ which corresponds to the domain of the image. We search for the restored image as the solution of the following minimization problem:

$$\inf_I \underbrace{\int_\Omega (I-N)^2 d\Omega}_{\texttt{term 1}} + \alpha \underbrace{\int_\Omega \phi(|\nabla I|) d\Omega}_{\texttt{term 2}} \tag{1}$$

where α is a constant and ϕ is a function still to be defined. Notice that if $\phi(x) = x^2$, we recognize the *Tikhonov* regularization term. How can we interpret this minimization? In fact, we search for the function I which will be simultaneously close to the initial image N and smooth (since we want the gradient as small as possible). However, this method is well known to smooth the image isotropically without preserving discontinuities in intensity. The reason is that with the quadratic function, gradients are too much penalized. One solution to prevent the destruction of discontinuities but allows for isotropically smoothing uniform areas, is to change the above quadratic term [10, 5, 4]. The key idea is that for low gradients, isotropic smoothing is performed, and for high gradient, smoothing is only applied in the direction of the isophote and not across it. This condition can be mathematically formalized if we look at the Euler-Lagrange equation (2), associated to energy (1):

$$2(I-N) - \alpha div \left(\frac{\phi'(\mid \nabla I \mid)}{\mid \nabla I \mid} \nabla I \right) = 0 \tag{2}$$

Let us concentrate on the regularization part associated to the `term 2` of (1). If we note $\eta = \frac{\nabla I}{|\nabla I|}$, and ξ the normal vector to η, we can show that:

$$div \left(\frac{\phi'(\mid \nabla I \mid)}{\mid \nabla I \mid} \nabla I \right) = \underbrace{\frac{\phi'(\mid \nabla I \mid)}{\mid \nabla I \mid}}_{c_\xi} I_{\xi\xi} + \underbrace{\phi''(\mid \nabla I \mid)}_{c_\eta} I_{\eta\eta} \tag{3}$$

where $I_{\eta\eta}$ (respectively $I_{\xi\xi}$) denotes the second order derivate in the direction η (respectively ξ). If we want a good restoration as described before, we would like to have the following properties:

$$\lim_{|\nabla I|\to 0} c_\eta = \lim_{|\nabla I|\to 0} c_\xi = \alpha > 0 \tag{4}$$

$$\lim_{|\nabla I|\to \infty} c_\eta = 0 \quad \text{and} \quad \lim_{|\nabla I|\to \infty} c_\xi = \beta > 0 \tag{5}$$

If c_ξ and c_η are defined as in (3), it appears that the two conditions of (5) can never be verified simultaneously. So, we will only impose for high gradients [10, 5, 4]:

$$\lim_{|\nabla I|\to\infty} c_\eta = \lim_{|\nabla I|\to\infty} c_\xi = 0 \quad \text{and} \quad \lim_{|\nabla I|\to\infty} \left(\frac{c_\eta}{c_\xi}\right) = 0 \tag{6}$$

Many functions ϕ have been proposed in the literature that comply to the conditions (4) and (6) (see [11]). From now on, ϕ will be a convex function with linear growth at infinity which verify conditions (4) and (6). In that case, existence and unicity of problem (1) has recently been shown in the space of functions of bounded variations [5].

2.2 The half quadratic minimization

The key idea is to introduce a new functional which, although defined over an extended domain, has the same minimum in I as (1) and can be manipulated with linear algebraic methods. The method is based on a theorem inspired from *Geman* and *Reynolds* [14]. If a function $\phi(.)$ complies with some hypotheses, it can be written in the form:

$$\phi(x) = \inf_d (dx^2 + \psi(d)) \tag{7}$$

where d will be called the dual variable associated to x, and where $\psi(.)$ is a strictly convex and decreasing function. We can verify that the functions ϕ such that (4) (6) are true permit to write (7). Consequently, the problem (1) is now to find I and its dual variable d_I minimizing the functional $\mathcal{F}(I, d_I)$ defined by:

$$\mathcal{F}(I, d_I) = \int_\Omega (I - N)^2 d\Omega + \alpha \int_\Omega d_I |\nabla I|^2 + \psi(d_I) d\Omega \tag{8}$$

It is easy to check that for a fixed I, the functional $\mathcal{F}$ is convex in d_I and for a fixed d_I, it is convex in I. These properties are used to perform the algorithm which consists in minimizing alternatively in I and d_I:

$$I^{n+1} = \underset{I}{\text{argmin}} \quad \mathcal{F}(I, d_I^n) \tag{9}$$

$$d_B^{n+1} = \underset{d_I}{\text{argmin}} \quad \mathcal{F}(I^{n+1}, d_I) \tag{10}$$

To perform each minimization, we simply solve the Euler-Lagrange equations, which can be written as:

$$I^{n+1} - N - \alpha div(d_I^n \nabla I^{n+1}) = 0 \tag{11}$$

$$d_I^{n+1} = \frac{\phi'(|\nabla I^{n+1}|)}{|\nabla I^{n+1}|} \tag{12}$$

Notice that equation (12) gives explicitly d_I^{n+1} while for (11), for a fixed d_I^n, I^{n+1} is the solution of a linear equation. After discretizing in space, we have that $(I_{i,j}^{n+1})_{(i,j)\in\Omega}$ is solution of a linear system which is solved iteratively by the Gauss-Seidel method for example. To obtain this linear system, the difficulty is to discretize the divergence term. We propose below an extension of an existing method which has the advantage of taking into account all the neighborhoods.

2.3 On discretizing the *divergence operator*

Let d and A given at nodes (i,j). The problem is to have an approximation of $div(d\nabla A)$ at the node (i,j). We denote by $\triangle^x$ and $\triangle^y$ the finite difference operators defined by:

$$\begin{aligned}\triangle^x A_{i,j} &= A_{i+\frac{1}{2},j} - A_{i-\frac{1}{2},j}\\ \triangle^y A_{i,j} &= A_{i,j+\frac{1}{2}} - A_{i,j-\frac{1}{2}}\end{aligned}$$

Using that notation, Perona and Malik [26] proposed the following approximation:

$$\begin{aligned} div(d\nabla A)_{i,j} &= \frac{\partial}{\partial x}\left(d\frac{\partial A}{\partial x}\right) + \frac{\partial}{\partial y}\left(d\frac{\partial A}{\partial y}\right) \approx \triangle^x(d\triangle^x A_{i,j}) + \triangle^y(d\triangle^y A_{i,j})\\ &\approx \begin{pmatrix} 0 & d_{i,j+\frac{1}{2}} & 0\\ d_{i-\frac{1}{2},j} & -S^P & d_{i+\frac{1}{2},j}\\ 0 & d_{i,j-\frac{1}{2}} & 0\end{pmatrix} \star A_{i,j} \end{aligned} \tag{13}$$

where the symbol $\star$ denotes the convolution and S^P is the sum of the four weights in the principal directions. Notice that we need to know the function d at intermediate nodes which can be computed by interpolation (see [26]). Our aim is to extend this approximation so that we could take into account the values of A at the diagonal nodes:

$$\begin{aligned} div(d\nabla A)_{i,j} = \alpha_P &\begin{pmatrix} 0 & d_{i,j+\frac{1}{2}} & 0\\ d_{i-\frac{1}{2},j} & -S^P & d_{i+\frac{1}{2},j}\\ 0 & d_{i,j-\frac{1}{2}} & 0\end{pmatrix} \star A_{i,j}\\ + \alpha_D &\begin{pmatrix} d_{i-\frac{1}{2},j+\frac{1}{2}} & 0 & d_{i+\frac{1}{2},j+\frac{1}{2}}\\ 0 & -S^D & 0\\ d_{i-\frac{1}{2},j-\frac{1}{2}} & 0 & d_{i+\frac{1}{2},j-\frac{1}{2}}\end{pmatrix} \star A_{i,j} \end{aligned} \tag{14}$$

where α_P and α_D are two weights to be discussed, and S^D is the sum of the four weights in the diagonal directions. Approximation (14) is consistent if and only if:

$$\alpha_P + 2\alpha_D = 1 \tag{15}$$

Now, there remains one degree of freedom. Two possibilities have been considered:

$$(\alpha_P, \alpha_D) = \text{ constant and for instance } = (\tfrac{1}{2}, \tfrac{1}{4}) \tag{16}$$

$$(\alpha_P, \alpha_D) = \text{ functions depending on } d \text{ (See figure 1)} \tag{17}$$

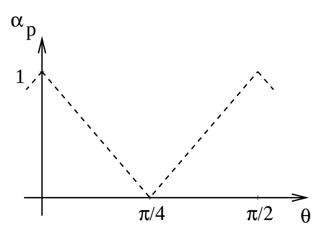

Figure 1: $\alpha_P = \alpha_P(\theta)$ is a $\pi/2$ periodic function where θ is the direction of the gradient of d. Notice that α_D can be deduced from the consistency condition is then computed thanks to the consistency condition (15)

We tested these different discretizations using quantitative measures. We checked that (14) permits to restore identically edges in principal or diagonal directions. Moreover, we observed that choosing α_P adaptatively (17) gave more precise results than (16). We will use the former approximation in the sequel.

3 The case of noisy images sequences

Let $N(x, y, t)$ denotes the noisy images sequence for which the background is assumed to be static. A simple moving object detector can be obtained using a thresholding technique over the *inter-frame difference* between a so-called *reference image* and the image being observed. Decisions can be taken independently point by point [12], or over blocks in order to achieve robustness in noise influence [32]. More complex approaches can also be used [25, 1, 16, 21, 6, 17, 18, 15, 13, 23]. However, in our application, we are not just dealing with a motion segmentation problem neither just a restoration problem. In our case, the so-called *reference image* is built at the same time while observing the image sequence. Also, the motion segmentation and the restoration are done in a coupled way, allowing the motion segmentation part to positively influence the restoration part and vice-versa. This is the key of our approach that allows to deal simultaneously with the problem of restoration and motion segmentation.

Section 3.1 formulates the continuous problem, in terms of a minimization problem which will be justified. In section 3.2, we rewrite the problem considering a finite number of images. The existence of a solution will be proved in a suitable space. Finally, we propose in section 3.3 the minimization algorithm based on the half quadratic minimization (see section 2). We will demonstrate that the discrete algorithm is unconditionally stable.

3.1 An optimization problem

Let $N(x,y,t)$ denotes the noisy images sequence for which the background is assumed to be static. Let us describe the unknown functions and what we would like them ideally to be:

(i) $B(x,y)$, the restored background,

(ii) $C(x,y,t)$, the sequence which will indicate the moving regions. Typically, we would like that $C(x,y,t)=0$ if the pixel (x,y) belongs to a moving object at time t, and 1 otherwise.

Our aim is to find a functional depending on $B(x,y)$ and $C(x,y,t)$ so that the minimizer verifies previous statements. We propose to solve the following problem:

Problem 1. Let $N(x,y,t)$ given. We search for $B(x,y)$ and $C(x,y,t)$ as the solution of the following minimization problem:

$$\inf_{B,C}\Big(\underbrace{\int_t\int_\Omega C^2(B-N)^2 d\Omega dt}_{\texttt{term 1}} + \underbrace{\alpha_c \int_t\int_\Omega (C-1)^2 d\Omega dt}_{\texttt{term 2}} \\ \underbrace{+\,\alpha_b^r \int_\Omega \phi_1(|\nabla B|)d\Omega + \alpha_c^r \int_t\int_\Omega \phi_2(|\nabla C|)d\Omega dt}_{\texttt{term 3}}\Big) \tag{18}$$

where ϕ_1 and ϕ_2 are convex functions that comply conditions (4) and (6) , and $\alpha_c, \alpha_b^r, \alpha_c^r$ are positive constants.

Getting the minimum of the functional means that we want each term to be small, having in mind the phenomena of the compensations.

The `term 3` is a regularization term. Notice that the functions ϕ_1,ϕ_2 have been chosen as in section 2 so that discontinuities may be kept.

If we consider the `term 2`, this mean that we want the function $C(x,y,t)$ to be close to one. In our interpretation, this means that we give a preference to the background. This is physically correct since the background is visible most of the time. However, if the data $N(x,y,t)$ is too far from the supposed background $B(x,y)$ at time t, then the difference $(B(x,y)-N(x,y,t))^2$ will be high, and to compensate this value, the minimization process will force $C(x,y,t)$ to be zero. Therefore, the function $C(x,y,t)$ can be interpretated as a movement detection function. Moreover, when searching for $B(x,y)$, we will not take into account $N(x,y,t)$ if $C(x,y,t)$ is small (`term 1`). This exactly means that $B(x,y)$ will be the restored image of the static background.

3.2 The temporal discretized problem

In this section, we present the discretized version in time of the problem 1. For a sequence $S(x,y,t)$, we will denote by $S_1(x,y),..,S_T(x,y)$ the associated T images. To simplify notations, we will often omit to write the coordinates (x,y). Discretizing in time $N(x,y,t)$ and $C(x,y,t)$ permits to rewrite the problem 1 in the following form:

Problem 2. Let $N_1,..,N_T$ be the noisy sequence. We search for B and $C_1,..,C_T$ as the solution of the following minimization problem:

$$\inf_{B,C_1,..,C_T} \Big(\underbrace{\sum_{h=1}^{T} \int_\Omega C_h^2 (B - N_h)^2 d\Omega}_{\texttt{term 1}} + \underbrace{\alpha_c \sum_{h=1}^{T} \int_\Omega (C_h - 1)^2 d\Omega}_{\texttt{term 2}}$$
$$+ \underbrace{\alpha_b^r \int_\Omega \phi_1(|\nabla B|) d\Omega + \alpha_c^r \sum_{h=1}^{T} \int_\Omega \phi_2(|\nabla C_h|) d\Omega}_{\texttt{term 3}} \Big) \tag{19}$$

The existence of a solution to the problem 2 can be proved in the space of bounded variations.

3.3 The minimization algorithm

This section is devoted to the numerical study of the problem 2. If we try to solve directly the Euler-Lagrange equations associated to (19), we will have to cope with non linear equation. To avoid this difficulty, we are going to use the same techniques as developed in the section 2.2. The idea is to introduce dual variables as defined in (7) each time it is necessary. This is the case for the $T+1$ restoration terms (`term 3`). Consequently, we introduce the $T+1$ dual variables noted d_B,($d_{C_1},..,d_{C_T}$) associated respectively to B,$C_1,..,C_T$. Using same arguments as in section 2.2, we will solve, instead of problem 2, the following problem:

Problem 3. Let $N_1,..,N_T$ the noisy sequence. We search for B,d_B, $C_1,..,C_T$ and $d_{C_1},..,d_{C_T}$

as the solution of the following minimization problem:

$$\inf_{B,C_1,..,C_T} \Big(\sum_{h=1}^{T} \int_\Omega \left[C_h^2 (B - N_h)^2 d\Omega + \alpha_c (C_h - 1)^2 \right] d\Omega$$
$$+ \alpha_b^r \int_\Omega \left[d_B |\nabla B|^2 d\Omega + \Psi_1(d_B) \right] d\Omega$$
$$+ \alpha_c^r \sum_{h=1}^{T} \int_\Omega \left[d_{C_h} |\nabla C_h|^2 d\Omega + \Psi_2(d_{C_h}) \right] d\Omega \Big) \tag{20}$$

We will note in the sequel $\mathcal{E}(B, d_B, C_h, d_{C_h})$ the corresponding functional. The main observation is that the functional $\mathcal{E}$ is quadratic with respect to B,$C_1, .., C_T$, and convex with respect to d_B and $(d_{C_h})_{h=1..T}$. Once initial conditions $(B^0, d_B^0, C_h^0, d_{C_h}^0)$ given, we compute the following system iteratively:

$$B^{n+1} = \underset{B}{\operatorname{argmin}} \quad \mathcal{E}(B, d_B^n, C_h^n, d_{C_h}^n) \tag{21}$$
$$d_B^{n+1} = \underset{d_B}{\operatorname{argmin}} \quad \mathcal{E}(B^{n+1}, d_B, C_h^n, d_{C_h}^n) \tag{22}$$
$$C_h^{n+1} = \underset{C_h}{\operatorname{argmin}} \quad \mathcal{E}(B^{n+1}, d_B^{n+1}, C_h, d_{C_h}^n) \tag{23}$$
$$d_{C_h}^{n+1} = \underset{d_{C_h}}{\operatorname{argmin}} \quad \mathcal{E}(B^{n+1}, d_B^{n+1}, C_h^{n+1}, d_{C_h}) \tag{24}$$

Equalities (23)-(24) are written for $h = 1..T$ The way to obtain each variable like described in (21)-(24) consists in solving the associated Euler-Lagrange equations. As we are going to see, the dual variables d_B^{n+1} and $(d_{C_h}^{n+1})_{h=1..T}$ are given explicitly, while B^{n+1} and $(C_h^{n+1})_{h=1..T}$ are solutions of linear systems. This linear systems will be solved by an iterative method like Gauss-Seidel's. Equations are:

$$\sum_{h=1}^{T} C_h^{n2} (B^{n+1} - N_h) - \alpha_B^r div(d_B^n \nabla B^{n+1}) = 0 \tag{25}$$
$$d_B^{n+1} = \frac{\phi_1'(|\nabla B^{n+1}|)}{|\nabla B^{n+1}|} \tag{26}$$
$$C_h^{n+1} \left[\alpha_C + (B^{n+1} - N_h)^2 \right] - \alpha_C - 2\alpha_C^r div(d_{C_h}^n \nabla C_h^{n+1}) = 0 \tag{27}$$
$$d_{C_h}^{n+1} = \frac{\phi_2'(|\nabla C_h^{n+1}|)}{|\nabla C_h^{n+1}|} \tag{28}$$

Remark that if $\alpha_C^r = 0$, $(C_h^{n+1})_{h=1..T}$ is in fact obtained by:

$$C_h^{n+1} = \frac{\alpha_C}{\alpha_C + (B^{n+1} - N_h)^2}$$

As for the linear systems (25) and (27), we discretized the divergence terms $div(d\nabla A)$ using the same technique as described in section 2.2.

3.4 An unconditionally stable algorithm

In this section, we prove that the discretized algorithm is unconditionally stable. This is expressed in the following proposition.

Proposition Let Ω^d be the set of pixels (i,j) in Ω and let $\mathcal{G}^d$ be the space of functions $(B, C_1, .., C_T)$ such that, for all pixels $(i,j) \in \Omega^d$ we have:

$$m_B \leq B \leq M_B \tag{29}$$

$$0 \leq C_h \leq 1 \qquad \text{for } h = 1..T \tag{30}$$

$$0 < m_C \leq \sum_{h=1}^{T} C_h \leq T \tag{31}$$

$$\text{where } \left\{ \begin{array}{l} m_B = \inf_{\substack{(x,y)\\ h=1..T}} N_h(x,y) \\ M_B = \sup_{\substack{(x,y)\\ h=1..T}} N_h(x,y) \end{array} \right. , \qquad m_C = \frac{T\alpha_c^r}{\alpha_c + (M_B - m_B)^2 + 4} \tag{32}$$

Then, for a given $(B^n, C_1^n, .., C_T^n)$ in $\mathcal{G}^d$, there exists a unique $(B^{n+1}, C_1^{n+1}, .., C_T^{n+1})$ in $\mathcal{G}^d$ such that (25)-(28) are satisfied. ■

Proof We first rewrite equations (21) (23) taking into account (26) (28):

$$\sum_{h=1}^{T} C_{h\,i,j}^{n\,2}(B_{i,j}^{n+1} - N_{h\,i,j}) - \alpha_B^r div\left(\frac{\phi_1'(|\nabla B^n|)}{|\nabla B^n|}\nabla B^{n+1}\right)_{i,j} = 0 \tag{33}$$

$$C_{h\,i,j}^{\,n+1}\left[\alpha_C + (B_{i,j}^{n+1} - N_{h\,i,j})^2\right] - \alpha_C - \alpha_C^r div\left(\frac{\phi_2'(|\nabla C_h^n|)}{|\nabla C_h^n|}\nabla C_h^{n+1}\right)_{i,j} = 0 \tag{34}$$

We now write the discretized equations in space. To this end techniques developed in section 2.2 can be used. Anyway, we will use the following notation:

$$div\left(\frac{\phi'(|\nabla A^n|)}{|\nabla A^n|}\nabla A^{n+1}\right)_{i,j} \approx$$

$$\sum_{(k,l)\in D} p_{i+k,j+l}(A^n)A_{i,j}^{n+1} - \left(\sum_{(k,l)\in D} p_{i+k,j+l}(A^n)\right) A_{i,j} \tag{35}$$

where $D = \{(k,l) \neq 0 \in [-1,0,1]^2\}$ and $(p_{i+k,j+l})_{(k,l)\in D}$ verify:

$$0 \leq p_{i+k,j+l} \leq 1 \qquad \text{and} \qquad \sum_{(k,l)\in D} p_{i+k,j+l} \leq 4 \tag{36}$$

Using this notation, and after some basic computation, we can re-write (33)-(34) in the following form:

$$B^{n+1}_{i,j} = \sum_{(k,l)\in D} \left(\frac{\alpha^r_B p_{i+k,j+l}(B^n)}{\sum_{h=1}^T {C^n_h}^2 + \alpha^r_B \sum_{(k,l)\in D} p_{i+k,j+l}(B^n)} \right) B^{n+1}_{i+k,j+l} + \sum_{h=1}^{T} \frac{N_h {C^n_h}^2_{i,j}}{\sum_{h=1}^T {C^n_h}^2_{i,j} + \alpha^r_B \sum_{(k,l)\in D} p_{i+k,j+l}(B^n)} \tag{37}$$

$$C_h{}^{n+1}_{i,j} = \sum_{h=1}^{T} \left(\frac{\alpha^r_C p_{i+k,j+l}(C^n_h)}{\alpha_C + (B^n - N_h)^2_{i,j} + \alpha^r_C \sum_{(k,l)\in D} p_{i+k,j+l}(C^n_h)} \right) C^n_{h\, i+k,j+l} + \frac{\alpha_C}{\alpha_C + (B^n - N_h)^2_{i,j} + \alpha^r_C \sum_{(k,l)\in D} p_{i+k,j+l}(C^n_h)} \tag{38}$$

To simplify notations, let us denote by $U^n_{i,j} \in R^{T+1}$, the vector defined by:

$$U^n_{i,j} = (B^n_{i,j}, C_{1\,i,j}, .., C_{T\,i,j})^t$$

where the subscript denotes the transposition symbol. Let $(M_{i+k,j+l}(U^n))_{(k,l)\in D}$ be diagonal matrices in $R^{T+1} \times R^{T+1}$ and $R(U^n)_{i,j}$ be a R^{T+1} valued vector such that equations (37) (38) may be rewritten in the following form:

$$U^{n+1}_{i,j} = \sum_{(k,l)\in D} M_{i+k,j+l}(U^n) U^{n+1}_{i+k,j+l} + R(U^n)_{i,j}$$

Now, for $V \in \mathcal{G}^d$, we define the linear function $Q_V(Z)$ by:

$$\begin{aligned} &Q_V : \mathcal{G}^d \to R^{T+1} \\ &Q_V(Z) = \sum_{(k,l)\in D} M_{i+k,j+l}(V) Z_{i+k,j+l} + R(V)_{i,j} \end{aligned} \tag{39}$$

Then we can show that:

$$Q_V(\mathcal{G}^d) \subset \mathcal{G}^d \tag{40}$$

$$Q_V \text{ is a contractive function on } \mathcal{G}^d \tag{41}$$

The first statement can be deduce directly from relations (37)-(38) and the definition of $\mathcal{G}^d$. Let us demonstrate (41).

$$\begin{aligned} |Q_V(Z) - Q_V(Y)| &\leq \sum_{(k,l)\in D} \|M_{i+k,j+l}(V)\| \;\; |Z_{i+k,j+l} - Y_{i+k,j+l}| \\ &\leq \left(\sum_{(k,l)\in D} \|M_{i+k,j+l}(V)\| \right) |Z - Y|_\infty \\ &\leq K |Z - Y|_\infty \end{aligned}$$

where $\|\cdot\|$, $|\cdot|$ and $|\cdot|_\infty$ correspond to usual norms, and K is a constant, independent of V and i, j, k, l which is greater than all the coefficients of the diagonal matrices $M_{i+k,j+l}(U)$ but strictly inferior to 1. More precisely, we can establish that:

$$K = sup\left\{\frac{4\alpha_B^r}{m_C + 4\alpha_B^r}, \frac{4\alpha_C^r}{\alpha_C + 4\alpha_C^r}\right\}$$

Consequently, thanks to the properties (40)-(41), we can apply the classical fixed point theorem to the function Q_V. So, for U^n in $\mathcal{G}^d$, there exist a unique $U^{n+1} \in \mathcal{G}^d$ such that:

$$U^{n+1} = Q_{U^n}(U^{n+1})$$

which is the fixed point of Q_{U^n}, that is to say U^{n+1} is the unique solution of (37)-(38). Moreover $U^{n+1} \in \mathcal{G}^d$. This concludes the proof. ■

4 Experiments

In this section, we present the results of applying our technique to restore noisy synthetic and real image sequences. We have tested our method on a number of image sequences and the obtained results have been very promising. Using noisy synthetic image allows us to quantify the improvements bring by our method with respect to more classical approaches. Figure 2 **(a)** shows a given frame extracted from the synthetic noisy image sequence produced to test the approach. We have superimposed some arrows on this image to illustrate the trajectories of each block in the image sequence. Figures 2 **c** and **d** shows the restored background using classical averaging or median filtering methods. To quantify the result, we have used the classical *Signal-to-Noise-Ratio* defined between an original image (I_1) and the restored image (I_2) by:

$$\mathrm{SNR}(I_1/I_2) = 10\log_{10}\left[\frac{\sigma^2(I_2)}{\sigma^2(I_1 - I_2)}\right]$$

We recall that the higher the SNR is, the better the restoration is.

SNR values related to figure 2 are reported in table 1.

The second example deals with a real image sequence. Figure 3 **(a.1)** shows one frame of the sequence and the different trajectories of the moving persons in the sequence. Two kind of results are presented. In figure 3, we essentially concentrate on the restoration part. See in particular how the background has been well restored by our method in 3 **(c)** and **c'** (moving object are correctly removed and discontinuities are preserved i.e no blur is introduced in the restoration process) and compare to fig (3 **(b)** and **b'**) where a simple averaging method has been used.

Figure 4 is concerned with the motion segmentation part. Two remarks can be done. Functions $(C_h)_{h=1..T}$, even if they are not exactly binary, permit an accurate motion segmentation. Furthermore, the dual functions $(d_{C_h})_{h=1..T}$, usually interpretated as edge detectors

I_2	SNR(I_1/I_2)	See figure 2
Noisy background (without objects)	9.5	**(b)**
Median image	5.7	**(c)**
Average image	9.8	**(d)**
Restored $B(x,y)$		
$\alpha_C^r = 0$	14.0	
$\alpha_C^r \neq 0$	14.4	**(e)**

Table 1: Results on a synthetic sequence (See figure 2). Image I_1 is the image of the clear background without any object.

for $(C_h)_{h=1..T}$, can then be seen as the boundaries of the moving regions. See in particular how accurate are these boundaries. They really correspond to the contours of the moving object in the considered frame i.e they do not correspond to the union of the contours detected in the considered and in the previous frame as usually done by most of the classical motion segmentation approaches. It is important to note also that in addition to the ability to detect the car and the 2 moving persons, we have also been able to detect the motion produced by the trees and the projected shadows on the ground floor.

5 Conclusion

We have presented in this article an original coupled method for the problem of image sequence restoration and motion segmentation. This original way to restore image sequence has been proved to give very promising result. To complete this work, the idea is to exploit information given by the motion segmentation part to restore also the moving regions. This is the object of our current work and hopefully we'll be able to show complete image sequence restoration at the time of the conference.

References

[1] T. Aach and A. Kaup. Bayesian algorithms for adaptive change detection in image sequences using markov random fields. *Signal Processing: Image Communication*, 7:147–160, 1995.

[2] L. Alvarez, P.-L. Lions, and J.-M. Morel. Image selective smoothing and edge detection by nonlinear diffusion (ii). *SIAM Journal of numerical analysis*, 29:845–866, 1992.

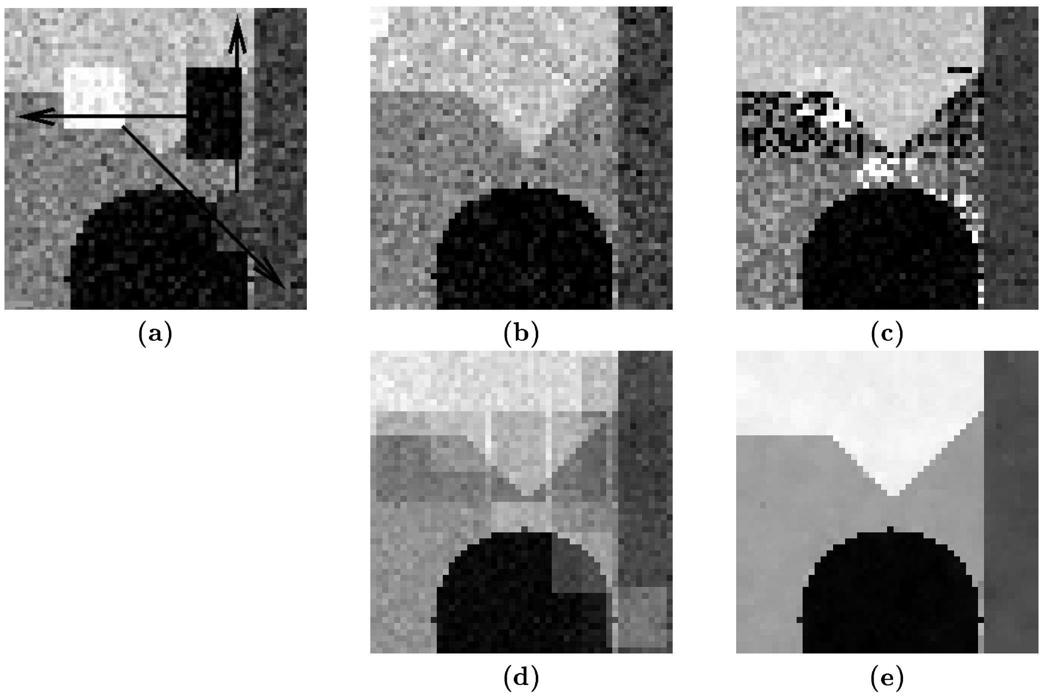

Figure 2: Results on a synthetic sequence (5 images) **(a)** One image of the sequence **(b)** Noisy background without objects **(c)** Median **(d)** Average **(e)** Restored background ($c \neq 0$). SNR values are reported in table 1

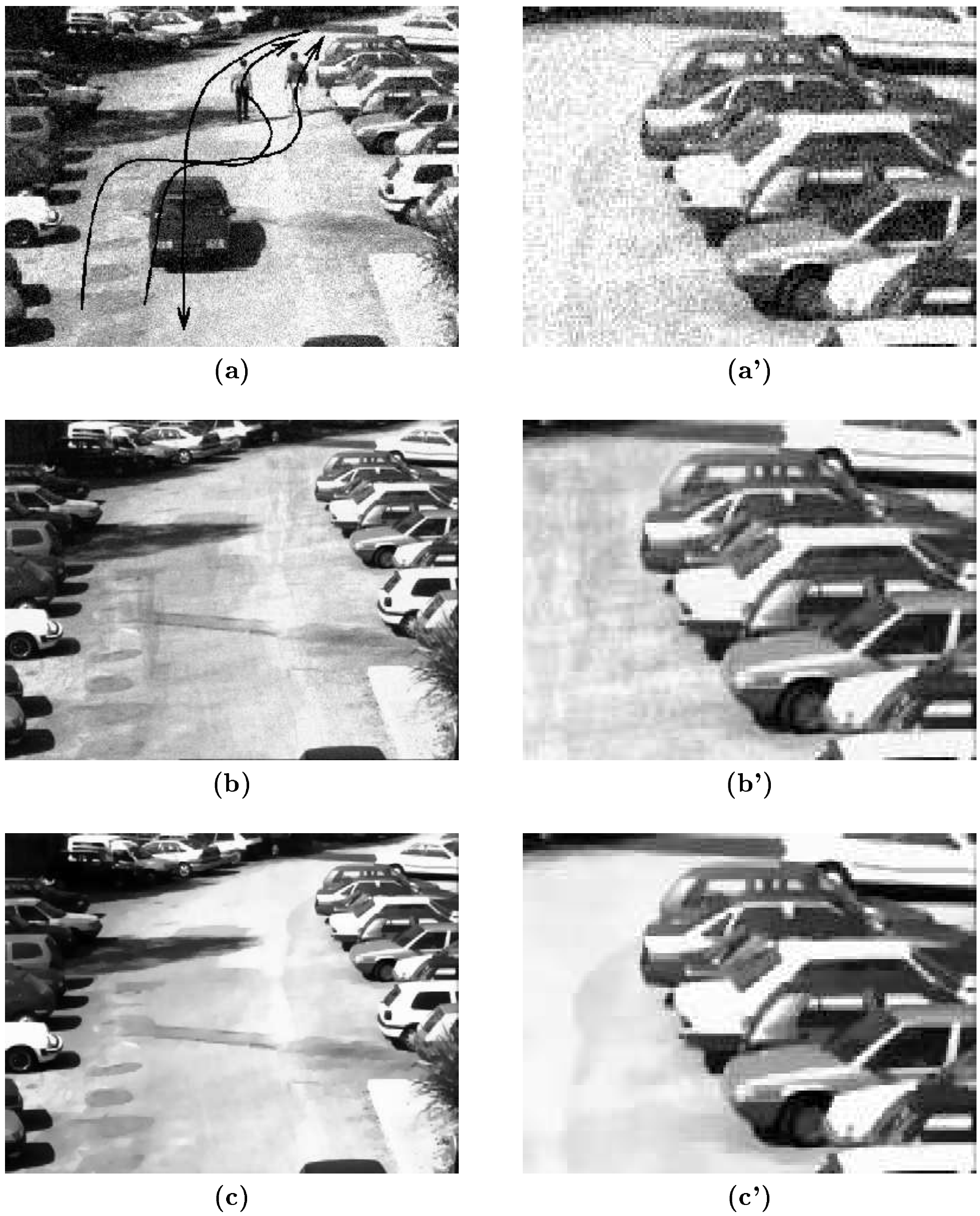

Figure 3: Results on a real sequence (12 images) `Left:` **(a)** One image of the sequence **(b)** Mean **(c)** Restored background $B(x, y)$ `Right:` Zoom on the left images to better compare the quality of the restoration.

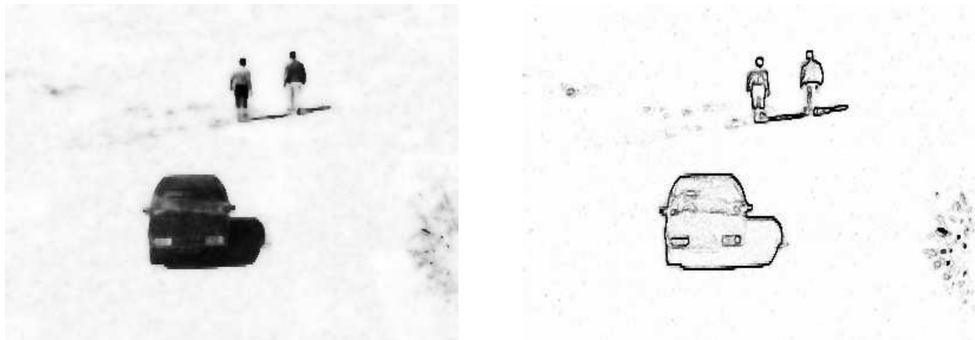

(a) (b)

Figure 4: Results concerning moving objects detection **(a)** Function $C(x, y, t)$ at a given time and **(b)** its dual variable associated d_C.

[3] L. Alvarez and L. Mazorra. Signal and image restoration using shock filters and anisotropic diffusion. *SIAM Journal of numerical analysis*, 31(2):590–605, Apr. 1994.

[4] G. Aubert, M. Barlaud, L. Blanc-Feraud, and P. Charbonnier. Deterministic edge-preserving regularization in computed imaging. *IEEE Trans. Imag. Process.*, 5(12), Feb. 1997.

[5] G. Aubert and L. Vese. A variational method in image recovery. *SIAM J. Numer. Anal.*, 34(5):1948–1979, Oct. 1997.

[6] J. Boyce. Noise reduction of image sequences using adaptative motion compensated frame averaging. In *IEEE ICASSP*, volume 3, pages 461–464, 1992.

[7] J. Brailean and A. Katsaggelos. Simultaneous recursive displacement estimation and restoration of noisy-blurred image sequences. *IEEE Transactions on Image Processing*, 4(9):1236–1251, Sept. 1995.

[8] O. Buisson, B. Besserer, S. Boukir, and F. Helt. Deterioration detection for digital film restoration. In *Computer Vision and Pattern Recognition*, pages 78–84, Puerto Rico, June 1997.

[9] L. D. Cohen. Auxiliary variables and two-step iterative algorithms in computer vision problems. *ICCV*, 1995.

[10] R. Deriche and O. Faugeras. Les EDP en traitement des images et vision par ordinateur. Technical report, INRIA, Nov. 1995. A more complete version of this Research Report

has appeared in the French Revue "Traitement du Signal". Volume 13 - No 6 - Special 1996.

[11] R. Deriche and O. Faugeras. Les EDP en Traitement des Images et Vision par Ordinateur. *Traitement du Signal*, 13(6), 1996.

[12] N. Diehl. Object-oriented motion estimation and segmentation in image sequences. *IEEE Transactions on Image Processing*, 3:1901–1904, Feb. 1990.

[13] E. Dubois and S. Sabri. Noise reduction in image sequences using motion-compensated temporal filtering. *IEEE Transactions on Communications*, 32(7):826–831, July 1984.

[14] D. Geman and G. Reynolds. Constrained restoration and the recovery of discontinuities. *IEEE Transactions on Pattern Analysis and Machine Intelligence*, 14(3):367–383, 1993.

[15] S. Geman, D. E. McClure, and D. Geman. A nonlinear filter for film restoration and other problems in image processing. *CVGIP : Graphical Models and Image Processing*, 54(4):281–289, July 1992.

[16] K. Karmann, A. Brandt, and R. Gerl. Moving object segmentation based on adaptive reference images. *Signal Processing: Theories and Applications*, V:951–954, 1990.

[17] A. Kokaram. Reconstruction of severely degraded image sequences. In *International Conference on Image Applications and Processing*, Florence, Italy, 1997.

[18] A. C. Kokaram and S. Godsill. A system for reconstruction of missing data in image sequences using sampled 3d ar models and mrf motion priors. In B. Buxton, editor, *Proceedings of the 4th European Conference on Computer Vision*, pages 613–624, Cambridge, UK, Apr. 1996.

[19] P. Kornprobst, R. Deriche, and G. Aubert. Image coupling, restoration and enhancement via PDE's. In *International Conference on Image Processing*, volume II of III, pages 458–461, Santa-Barbara,California, Oct. 1997.

[20] P. Kornprobst, R. Deriche, and G. Aubert. Nonlinear operators in image restoration. In *Proceedings of the International Conference on Computer Vision and Pattern Recognition*, pages 325–331, Puerto-Rico, June 1997. IEEE.

[21] S. Liou and R. Jain. Motion detection in spatio-temporal space. *Computer Vision, Graphics and Image Understanding*, (45):227–250, 1989.

[22] R. Malladi and J. Sethian. Image processing: Flows under min/max curvature and mean curvature. *Graphical Models and Image Processing*, 58(2):127–141, Mar. 1996.

[23] R. Morris. *Image Sequence Restoration using Gibbs Distributions.* PhD thesis, Cambridge University, England, 1995.

[24] N. Nordström. Biased anisotropic diffusion - a unified regularization and diffusion approach to edge detection. *Image and Vision Computing*, 8(11):318–327, 1990.

[25] N. Paragios and G. Tziritas. Detection and localization of moving objects in image sequences. *FORT-Hellas Technical Report, Accepted for publication in Signal Processing: Image Communication*, Oct. 1996.

[26] P. Perona and J. Malik. Scale-space and edge detection using anisotropic diffusion. *IEEE Transactions on Pattern Analysis and Machine Intelligence*, 12(7):629–639, July 1990.

[27] M. Proesmans, E. Pauwels, and L. V. Gool. *Coupled Geometry-Driven Diffusion Equations for Low-Level Vision*, pages 191–228. Computational imaging and vision. Kluwer Academic Publishers, 1994.

[28] L. Rudin and S. Osher. Total variation based image restoration with free local constraints. In *International Conference on Image Processing*, volume I, pages 31–35, Nov. 1994.

[29] G. Sapiro, A. Tannenbaum, Y. You, and M. Kaveh. Experiments on geometric image enhancement. In *International Conference on Image Processing*, 1994.

[30] J. Shah. Segmentation by nonlinear diffusion. In *Proceedings of the International Conference on Computer Vision and Pattern Recognition*, pages 202–207, Lahaina, Hawai, June 1991. IEEE.

[31] J. Weickert. *Anisotropic Diffusion in Image Processing*. PhD thesis, University of Kaiserslautern, Germany, Laboratory of Technomathematics, Jan. 1996.

[32] O. Wenstop. Motion detection from image information. *Proceedings in Scandianvian Conference on Image Analysis*, pages 381–386, 1983.

[33] Y. You, M. Kaveh, W. Xu, and A. Tannenbaum. Analysis and Design of Anisotropic Diffusion for Image Processing. In *International Conference on Image Processing*, volume II, pages 497–501, Nov. 1994.

Unité de recherche INRIA Sophia Antipolis
2004, route des Lucioles - B.P. 93 - 06902 Sophia Antipolis Cedex (France)

Unité de recherche INRIA Lorraine : Technopôle de Nancy-Brabois - Campus scientifique
615, rue du Jardin Botanique - B.P. 101 - 54602 Villers lès Nancy Cedex (France)
Unité de recherche INRIA Rennes : IRISA, Campus universitaire de Beaulieu - 35042 Rennes Cedex (France)
Unité de recherche INRIA Rhône-Alpes : 655, avenue de l'Europe - 38330 Montbonnot St Martin (France)
Unité de recherche INRIA Rocquencourt : Domaine de Voluceau - Rocquencourt - B.P. 105 - 78153 Le Chesnay Cedex (France)

Éditeur
INRIA - Domaine de Voluceau - Rocquencourt, B.P. 105 - 78153 Le Chesnay Cedex (France)
http://www.inria.fr
ISSN 0249-6399